sciendo

DOI 10.2478/ama-2023-0054

acta mechanica et automatica, vol.17 no.3 (2023)
Special Issue "Computational Technologies in Engineering TKI2022"

MODELLING OF THE VISCOSITY EFFECT OF HEAVE PLATES FOR FLOATING WIND TURBINES BY HYDRODYNAMIC COEFFICIENTS

Ewelina CIBA*, Paweł DYMARSKI**

*Faculty of Mechanical Engineering and Ship Technology, Gdansk University of Technology,
ul. Narutowicza 11/12 8-233 Gdansk, Poland

ewelina.ciba@pg.edu.pl, pawdymar@pg.edu.pl

received 27 February 2023, revised 18 April 2023, accepted 24 April 2023

Abstract: One of the methods of modelling the movement of floating wind turbines is the use of the diffraction method. However, this method does not take into account the influence of viscosity; therefore, in many cases, it needs to be extended with a matrix of appropriate coefficients. The effect of viscosity causes both the added mass coefficient and the damping coefficient to increase. The determined coefficients were entered into the ANSYS AQWA program, and the calculation results of the transfer function determined with the use of linear and quadratic damping were presented. The results were compared with the results of the experiment, indicating greater convergence for the quadratic model.

Key words: spar platforms, heave plates, hydrodynamic coefficient, floating offshore wind turbines (FOWTs)

1. INTRODUCTION

The topic of floating offshore wind turbines (FOWTs) is becoming increasingly popular. There are many different platform concepts, with the most popular being various modifications of the Spar concept, such as the cell-Spar concept presented by Dymarski et al. [1].

For conceptual work, a very good method of simulating the platform in sea conditions is software based on the diffraction method, e.g. the commercial ANSYS AQWA program. Determination of wave forces on a stationary support structure for offshore wind turbines using the ANSYS AQWA program was demonstrated by Kraskowski and Marcinkowski [2], resulting in very high convergence as determined based on the results of the experiment. The use of this program was also presented by Motallebi et al. [3], who performed analyses of the DeepCwind semi-submersible FOWT platform with a nonlinear multi-segment catenary mooring line and intermediate buoy. The research carried out is very promising for this type of anchorage. It was concluded that by correctly selecting the buoy volume and position along the cable, the tension of the cable may be reduced by up to 45%.

ANSYS AQWA allows the user to quickly compare different concepts and check the impact of the applied modifications. However, the diffraction method on which it is based does not take into account the effect of viscosity, which may be of key importance in some cases; so, it should be supplemented by adding a matrix of additional coefficients. The paper presents the method of determining these coefficients for three different constructions: a smooth cylinder, a cylinder with a full heave plate and heave plates with holes, using forced oscillation tests carried out through the RANSE-CFD method. Initial considerations and results of model tests for heave plates and heave plates with holes were presented by Ciba et al. [4].

The issue of heave plates has been discussed many times in the literature. Extensive analyses of the damping plate effects were conducted by Subbullakshmi and Sundaravadivelu [5]. The authors examined various plate configurations, with reference to their diameter and position and double plates. They noticed, among other things, that the damping effect of the plate increases when its diameter is increased to 1.4 times the diameter of the platform, and thereafter, it begins to decrease. This is confirmed by the conclusions drawn by Tao and Cai [6]. They analysed vortex structures around a heave plate cylinder of different diameters. The research shows that the vortices flowing from the edge of the plate cannot be located too far from the cylinder surface, because then the damping is lower.

Medina-Manuel et al. [7] conducted model studies of a heave plate cylinder with a large plate diameter to cylinder diameter ratio (Dhp/D ~ 2.9) in a wide range, changing both the motion amplitude and the excitation frequency. Using two methods, forced and free oscillations, they determined the values of the hydrodynamic coefficients of the tested plate. They presented the results on graphs depending on the number of Keulegan–Carpenter (KC) and β, giving the basis for estimating their size for other cases of interest to the reader.

Analyses presented by Ciba [8] showed that even residual heave plates significantly increase attenuation. This leads to the conclusion that the damping value is most influenced by the edge of the plate and not its surface. Hence, the concept of perforated plates was initiated.

Research for the circular porous plate itself was carried out by Tao and Dray [9]. They determined the hydrodynamic characteristics of an oscillating porous disk. The tests were carried out for forced oscillations. They noticed that the added mass coefficient is lower for the porous plate and that, with the low KC related to the amplitude of the displacements, there is an increase in damping for the porous plates.

Perforated square plates were examined by An and Faltinsen [10]. The tests were also carried out for an insulated plate by means of forced oscillations. They also noticed a reduction in added mass through perforation. They also pointed out that at low KC numbers, damping is mainly due to fluid flow through the holes. Similar studies were carried out by Tian et al. [11]. They examined the hydrodynamic coefficients of heave plates using the forced oscillation method. The influences of the thickness ratio, shape, edge corner radius, perforation ratio and hole size on the hydrodynamic coefficients of a single plate were analysed and presented. For the twin- and triplet-plate configurations, the spacing effects were also evaluated. The test results confirm that the holes allow us to reduce added mass in relation to the full plate. They also confirm the observation that for small KC numbers (KC < 0.6), the damping coefficient of the plate with holes is greater than that of the solid plate. Mentzori and Kristiansen [12] presented interesting results of research and numerical simulations of hydrodynamic coefficients of two parallel perforated plates. They examined the influence of the distance between them on the nature of the flow and presented detailed visualisations of the tested cases. Based on the analyses, they indicate a tendency that a smaller distance between the plates gives greater attenuation. This is an interesting and promising concept, and further research in this area will be interesting. Molin [13] analysed perforated elements of various shapes, indicating potential applications in marine and offshore structures. In addition to heave plates, he also provided bilge keels, bodies that must be lifted down through the splash zone in a manner similar to mud mats and hatch covers. It confirms that porous structures are a good way to reduce inertial forces and slamming loads and to increase the damping of the resonant response.

For some time, the interest in the perforation of damping plates has been growing, which is a derivative of the growing interest in structures for offshore wind turbines. Mojtaba et al. [14] provided an extensive summary of damping plates. They noticed that the influence of the plates on the behaviour of the structure depends on the following parameters: the KC number, the frequency of oscillations, the ratio of perforations, the arrangement and size of cavitation, the thickness of the plate and its distance from the bottom and the free surface. They reported that at small numbers of KC, where the amplitude of the oscillations is limited, the viscous damping due to flow separation is proportional to the edge area. Hence, the addition of internal edges through perforation increases the viscous damping. So, they introduced an additional plate description factor: the ratio of the edge area to the plate area.

The method of determining the hydrodynamic coefficients by means of forced oscillations is slightly more troublesome than the method of free oscillations. However, it allows us to determine the value of the coefficients for different excitation frequencies, which is very important because in operating conditions the object will be exposed to waves of different frequencies. This was pointed out, among others, by Rao et al. [15]. They tested the coefficients of damping plates and compared the results with three different models of linear, quadratic and combined (quadratic with linear) damping, obtaining the best agreement for the linear model. This is contrary to the observations made by the authors further on within the present dissertation, but it may result from a greater number of KC of the analysed cases (KC ~ 2), which is related to the amplitude of the movement and has a large impact on the character of the flow around.

Useful calculations for modelling heave plates were made by Maron et al. [16]. They built one of the largest heave plate cylinder models ever studied to test the scale effect of this study. The conclusions from the conducted research are very useful for design, as they state that the hydrodynamic coefficients of heave plates depend mainly on the KC number, and the effect of the scale effect is small.

Experimental research and numerical analyses of the spar platform on a regular wave were carried out by Raed and Murali [17]. The calculations were made using the panel method with an additional damping matrix obtained using the free decay test. Against the backdrop of the results of the experiment, the aforementioned researchers compared the values and terms of the transfer function obtained for the model with only linear damping vis-à-vis those corresponding to quadratic damping, and observed that a better agreement was obtained in the case of the second of these. Determining the damping coefficients on the basis of forced oscillation tests would probably allow for even better agreement of results, although it is a more laborious method.

2. PURPOSE AND SCOPE OF THE RESEARCH

The present research aimed to compare a full heave plate and a heave plate with holes (Fig. 1), as an additional element for wind turbine platforms. For this purpose, the hydrodynamic coefficients for both structures were determined using the forced oscillation method (using RANSE-CFD calculations) and compared with each other. For comparison, coefficients for a smooth cylinder were also determined. Calculations were made for an excitation amplitude of $za = 0.02$ m and periods equal to $T = 0.6$ s, 0.8 s, 1.0 s, 1.2 s, 1.4 s, 1.6 s, 1.8 s and 2.0 s.

The determined coefficients were then introduced into the ANSYS AQWA program, thus supplementing the influence of viscosity, omitted in the diffraction method. Calculations of the behaviour of the structure on a regular wave were carried out using two methods: viscosity addition using the linear method and the quadratic method, using the Morison drag coefficient.

Based on the displacements of the structure in a regular wave, response amplitude operator functions were created and compared with the results of the experiment, and the results of the RANSE-CFD calculations are described by Ciba et al. [4].

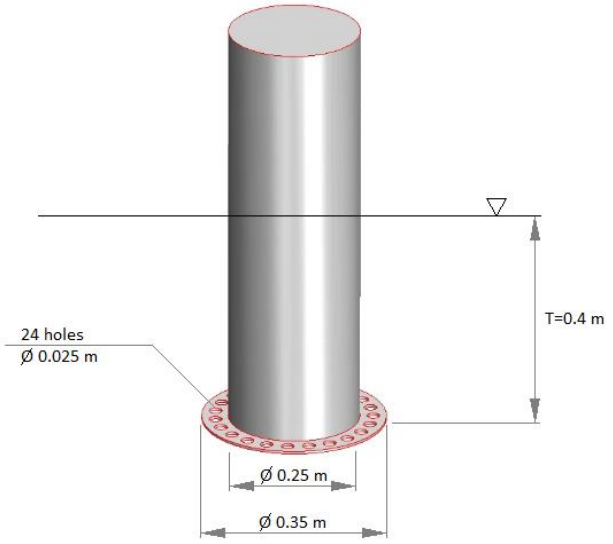

Fig. 1. Cylinder equipped with heave plates with holes

sciendo
DOI 10.2478/ama-2023-0054

3. MATHEMATICAL DESCRIPTION OF ISSUE

The forced oscillation test is carried out by causing the object (Eq. [1]) to oscillate. The in-phase excitation force component is related to inertia and stiffness, while the out-of-phase component is related to damping. Integrating the equation of motion (Eq. [1]), we obtain the velocity (Eq. [2]) and acceleration (Eq. [3]) of the object:

$$z(t) = z_a \sin\omega t \tag{1}$$

where

$$\dot{z} = z_a\, \omega \cos \omega t \tag{2}$$

$$\ddot{z} = -\, z_a\, \omega^2 \sin \omega t \tag{3}$$

Hence, the equation of forced motion (Eq. [4]) can be written as follows (Eq. [5]):

$$(m + a)\ddot{z} + b\dot{z} + cz = F_a \sin(\omega t + \varepsilon_{F_z}) \tag{4}$$

$$z_a\{-(m + a)\omega^2 + c\} \sin \omega t + z_a b\omega \cos\omega t = F_a \cos \varepsilon_{F_z} \sin \omega t + F_a \sin \varepsilon_{F_z} \cos \omega t \tag{5}$$

Hence, the hydrodynamic coefficient can be determined from the following relations: added mass *a* (Eq. [6]), damping coefficient b (Eq. [7]) and restoring force coefficient *c* (Eq. [8]):

$$dla\ \omega t = \frac{\pi}{2} : a = \frac{c - \frac{F_a}{z_a}\cos \varepsilon_{F_z}}{\omega^2} - m \tag{6}$$

$$dla\ \omega t = 0 : b = \frac{\frac{F_a}{z_a}\sin \varepsilon_{F_z}}{\omega} \tag{7}$$

based on geometry: $c = \rho g A_w$ (8)

The force components can be found by integrating the force over *N* number of cycles multiplied by $\cos \omega t$ i $\sin \omega t$, respectively:

$$F_a \sin \varepsilon_{F_z} = \frac{2}{NT}\int_0^{NT} F(t) \cdot \cos \omega t \cdot dt \tag{9}$$

$$F_a \cos \varepsilon_{F_z} = \frac{2}{NT}\int_0^{NT} F(t) \cdot \sin \omega t \cdot dt \tag{10}$$

Morison's Eq. (11) assumes that we can separate the force acting on the body into an acceleration component – the inertia term and a velocity component – the drag term.

$$F(t) = \frac{1}{2}\rho C_D A_p |W - \dot{z}|(W - \dot{z}) + \rho V_b(1 + C_a)\left[\frac{\partial W}{\partial t} + (U - \dot{z})\frac{\partial W}{\partial z}\right] - \rho V_b C_a \ddot{z} \tag{11}$$

where *F(t)* [N] is the force acting on the structure, ρ [kg/m^3] is water density, C_D [-] is Morison's drag coefficient, A_p [m^2] is the cross-sectional area, *W* [m/s] is the water velocity, $\dot{z}$ [m/s] is the speed of the structure, V_b [m^3] is the volume of the submerged part, C_a [-] is the added mass coefficient and $\ddot{z}$ [m/s^2] is the acceleration of the structure.

4. RANSE-CFD CALCULATIONS

CFD calculations were made using STAR-CCM+. Non-stationary calculations were performed in the three-dimensional domain, using the volume of fluid and K-epsilon turbulence models. By employing an overset mesh, it became possible to model cylinder displacements for a given motion trajectory. The computational domain measuring 4 m × 2 m × 2.25 m was prepared as indicated in Fig. 2.

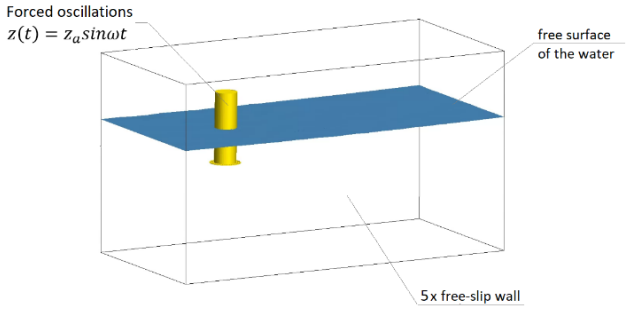

Fig. 2. Computational domain

The volume of water and air fractions for a plane wave was assumed as the initial condition. Slippery walls were placed on the walls of the field and on its bottom. From above, the domain was opened with the inlet condition with zero velocity by the volume of the air fraction.

An overset mesh was used (Fig. 3), consisting of a moving (green) and a fixed (black) part, allowing the simulation of the object's movement. The mesh was compacted near the free water surface, around the heave plate and in the area expected to move the cylinder. On the surface of the cylinder, an element size of 0.002 m from five prism layers with a total thickness of 0.002 m was applied. A mesh was obtained consisting of 1,281,102 cells in the movable portion and 1,282,998 in the fixed portion.

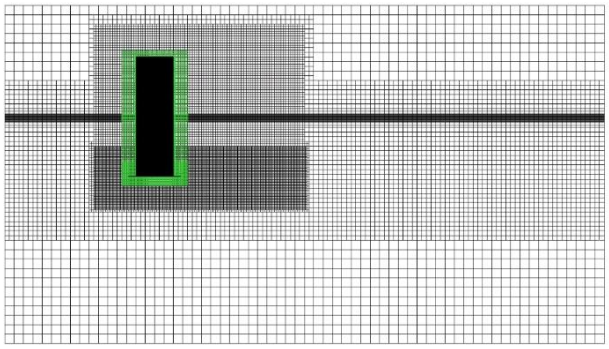

Fig. 3. Calculation grid in the symmetry plane divided into a movable (green) and a fixed (black) part

In order to ensure a thorough verification of the mesh, apart from the basic calculations performed in relation to the medium mesh characterised by 2,562,100 as the number of constituent elements, calculations were also performed on the coarse mesh (2,007,507) and the fine mesh (3,323,540); these calculations produced similar results, which are shown in Fig. 4, although these results do not count in terms of the ultimate conclusion gleaned from the present study.

Calculations were performed with time step t_k = 0.01 s. The vertical force on the structure was measured.

The validity of the time step was ascertained by repeating the calculations with a smaller t_k = 0.005 s and a larger t_k = 0.02 s time steps. The comparison of the results is shown in Fig. 5.

DOI 10.2478/ama-2023-0054

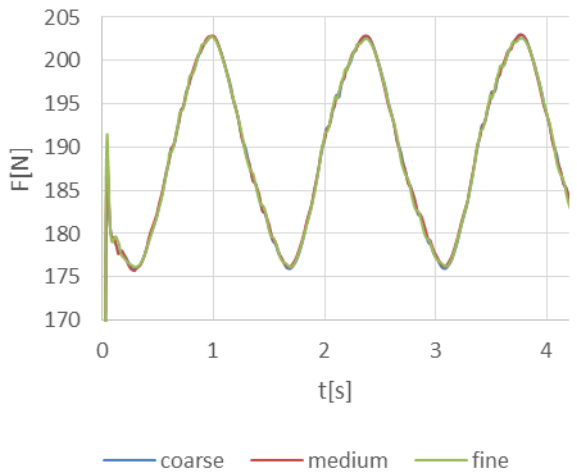

Fig. 4. Influence of the mesh density on the value of the calculated force

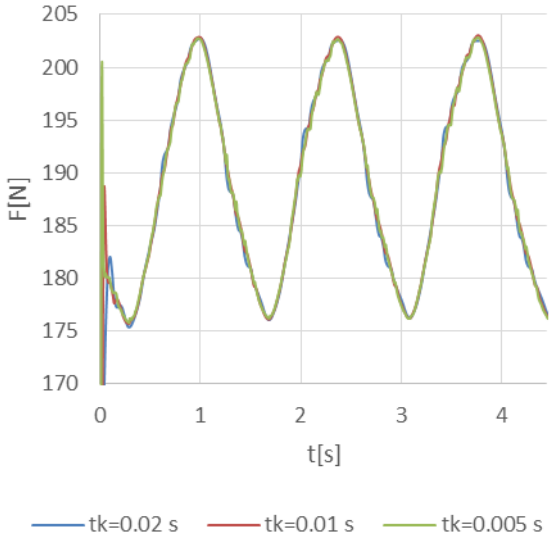

Fig. 5. The validity of the time step

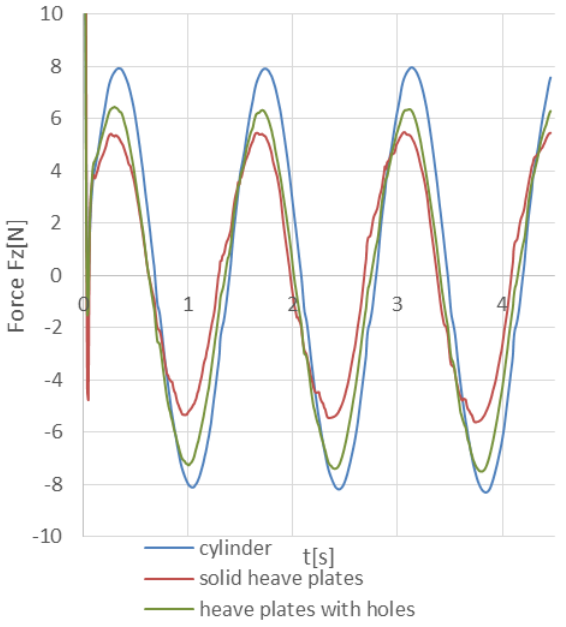

Fig. 6. Force on each of the three structures due to oscillatory excitation with period T = 1.4 s

An exemplary course of forces for oscillations with a period of $T = 1.4$ s for each of the three structures is shown in Fig. 6.

It may seem quite surprising that the largest force amplitude was obtained for a smooth cylinder. By way of offering an explanation for this, Fig. 7 shows the force distribution part related to inertia, damping and restoring force for a smooth cylinder.

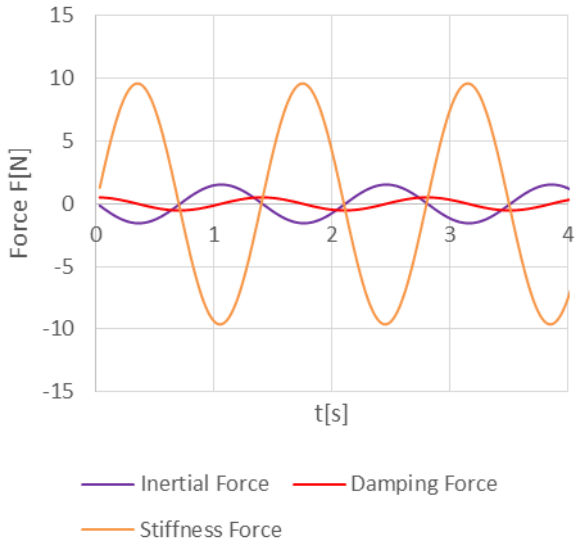

Fig. 7. Components of the force acting on a smooth cylinder

It can be seen from this that the stiffness force associated with the buoyancy of the structure has the largest share. The inertia force is in antiphase to it; hence, while the added mass of the smooth cylinder is the smallest, the net force acting on the cylinder will be the greatest.

In order to best analyse the properties of the structure, the waveforms of the inertia force (Fig. 8) and the damping forces (Fig. 9) for each of them have been shown. The course of the stiffness force is obviously the same because the waterline of each of them is the same.

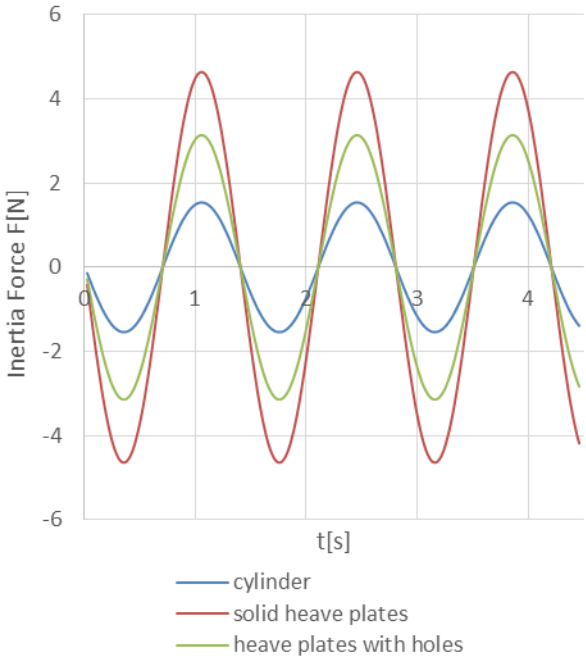

Fig. 8. Inertia force acting on the tested structures

sciendo
DOI 10.2478/ama-2023-0054
acta mechanica et automatica, vol.17 no.3 (2023)
Special Issue "Computational Technologies in Engineering TKI2022"

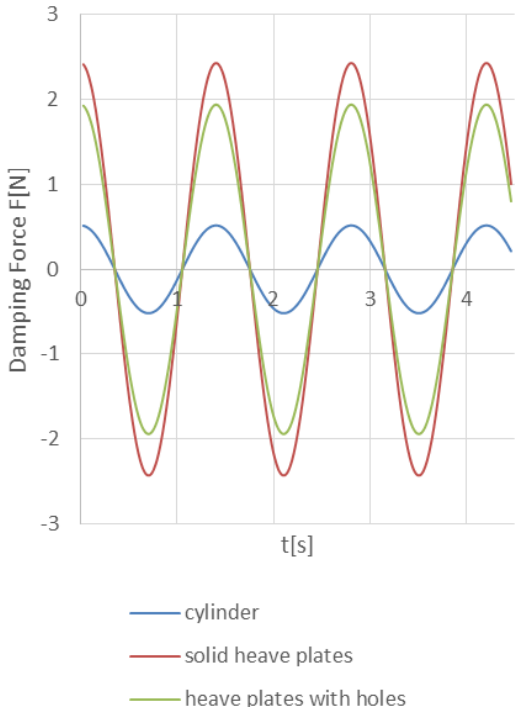

Fig. 9. The damping force acting on the tested structures

Analysing the data presented in the graphs, it is clear that the largest inertia force affects the structure with a solid damping plate, which is related to the largest added mass. The differences in the case of each of the three constructions are quite clear. In the case of the damping force, the differences between the solid plate and the plate with holes are not so large, although the force is clearly greater for the solid plate. From this, it can be concluded that the perforated plate causes quite a high damping without increasing the added mass as much as a solid plate, which in some cases can be very advantageous.

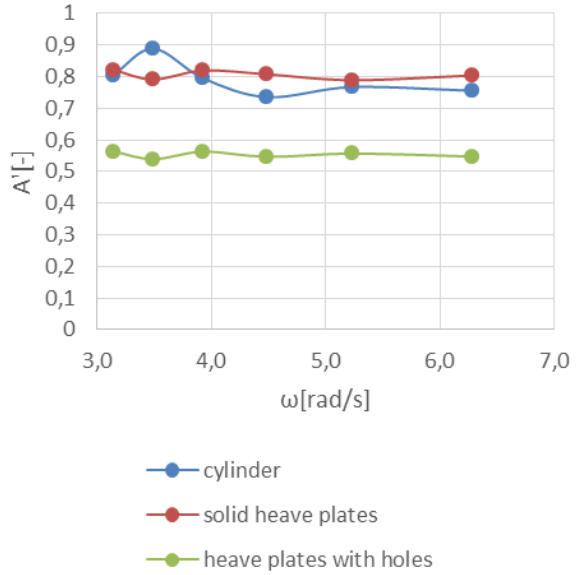

Fig. 10. Dimensionless added mass coefficient A´= a/m´

On the basis of the performed simulations, the hydrodynamic coefficients of the linear equation, the added mass a and the damping coefficient b were determined. To facilitate the analysis, the obtained values are presented in a dimensionless form, referring to the theoretical added mass for disc m´= 1/3ρD³, which is similar to the inference arrived at in the study of Tao and Dray [9], in which the following descriptions were given, that is to say, A´ = a/m´(Fig. 10) and B´= b/2mω (Fig. 11).

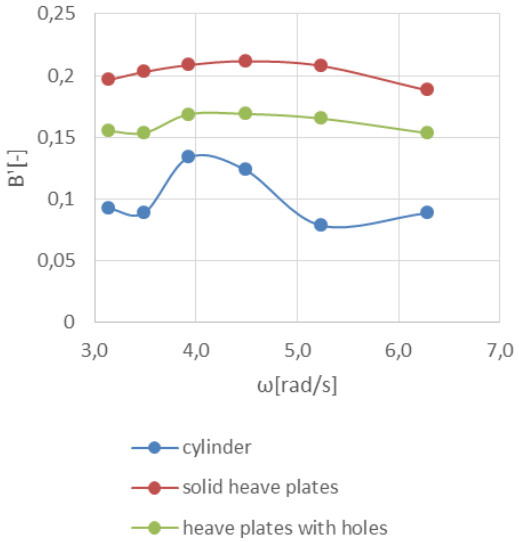

Fig. 11. Dimensionless damping coefficient B´= b/2mω

Based on the presented values, it is clear that a solid plate gives a greater added mass than a plate with holes. Also the damping coefficient is greater with a solid plate. Although this is not clearly visible after dimensioning, it should be emphasised that while the added mass does not change significantly depending on the oscillation period, in the case of the value of the damping coefficient, we observe a clear relationship: the longer the oscillation period, the lower the damping value.

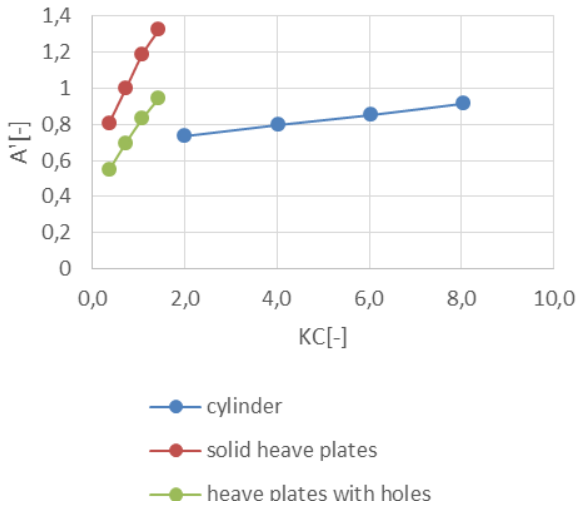

Fig. 12. Dimensionless added mass coefficient A´= a/m´dependent on KC. KC, Keulegan–Carpenter number

The assumption of linearity is actually a major simplification. It was therefore checked how the value of the determined coefficients changes depending on the amplitude of the movement. The results pertaining to the oscillation period $T = 1.4$ s are shown in Fig. 12 for dimensionless added mass and Fig. 13 for dimensionless damping coefficient.

DOI 10.2478/ama-2023-0054

The obtained values of the dimensionless added mass coefficients and the damping coefficient for the solid plate are close to those presented in the literature, e.g. as reported by Medina-Manuel et al. [7].

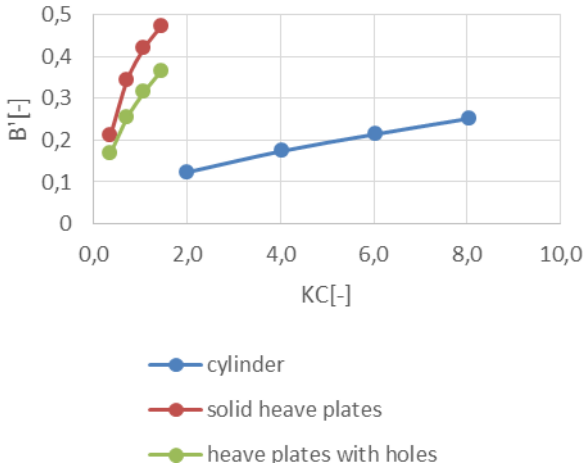

Fig. 13. Dimensionless damping coefficient B′= b/2mω dependent on KC. KC, Keulegan–Carpenter number

Based on the presented values, it can be concluded that the greater the excitation amplitude, the greater the value of both the added mass and the damping coefficient. This is a very important observation, especially in the context of determining the transfer function. If we want to obtain a high compliance of the maximum value of the transfer function with reality, we should select the damping coefficient for the expected displacement amplitude. However, it may then turn out that we will receive underestimated values in the remaining wave range.

An example of calculations of the force course using a linear equation with determined coefficients (dashed line) and the force calculated in the program for a cylinder with a solid plate (solid line) oscillating with a period of $T = 1.4$ s is shown in Fig. 14.

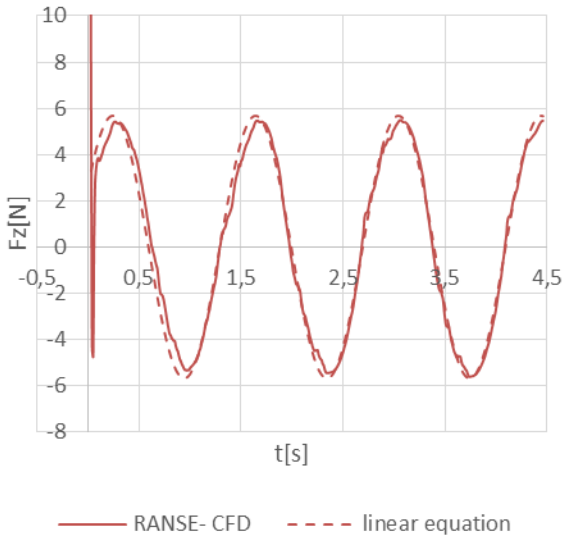

Fig. 14. Force on cylinder with solid heave plates

Using the method of least squares concomitant with employing the determined force values, the coefficients of the Morison equation were also determined for the tested cases. Their values are shown in Fig. 15 – drag coefficient CD and Fig. 16 – coefficient of added mass Ca. The values of the added mass coefficient were very similar to those determined on the basis of the added mass of the linear equation, which are marked on the graph with a dashed line.

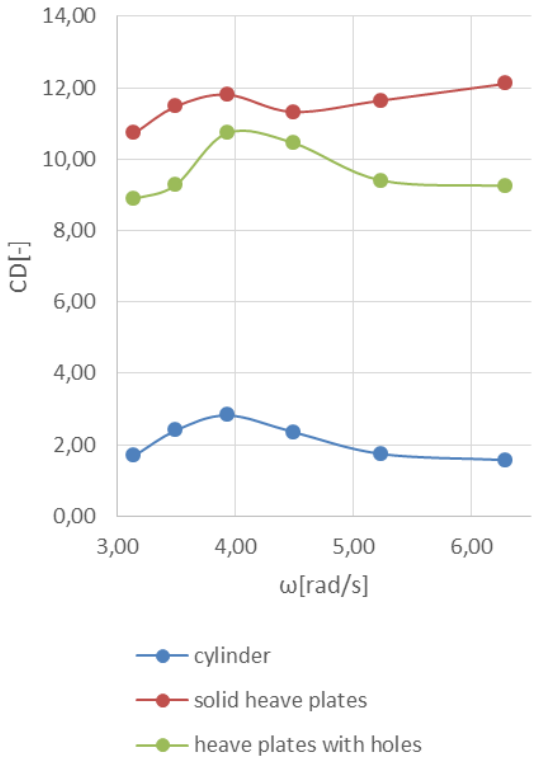

Fig. 15. Morison drag coefficient

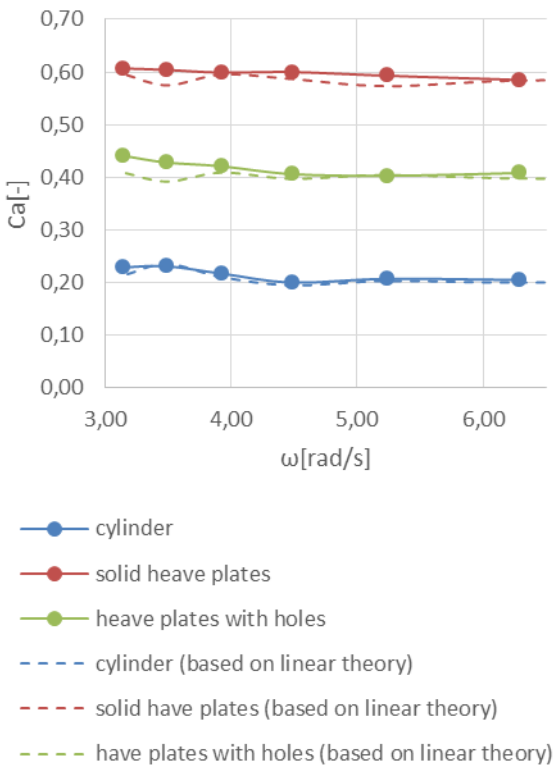

Fig. 16. Added mass coefficient

Based on the obtained results, the following conclusions can be drawn. Changes in the value of the drag coefficient depending on the oscillation period are not as large as in the case of the linear damping coefficient. This is very important from the point of view of viscosity modelling in the AQWA program because only a constant coefficient of additional drag is available there.

The values of the added mass coefficients determined by both methods are similar.

5. CALCULATIONS OF RESPONSE AMPLITUDE OPERATORS

In the case of analyses for floating objects, one of the key issues is to determine the transfer function, i.e. the response of the structure depending on the frequency of the excitation wave. It allows us to predict which waves pose the greatest threat to the safety of the structure, and by comparing it with the spectrum of an irregular wave, we can determine the expected actual displacement of the structure during its operation.

These functions for constructions with full heave plate and heave plate with holes were determined using various methods:

- an experiment;
- RANSE-CFD calculations;
- calculations using the diffraction method extended by linear drag coefficients (AQWA b); and
- calculations using the diffraction method extended by quadratic drag coefficients (AQWA CD).

The results, in the form of drawings, are presented in Fig. 17 for a solid plate and in Fig. 18 for a plate with holes.

It is clear that in the case of the diffraction method, much better results are obtained when the model is extended by quadratic rather than linear drag coefficients. This method gives results that are as good as, or even better than, those of the much more time-consuming RANSE-CFD method.

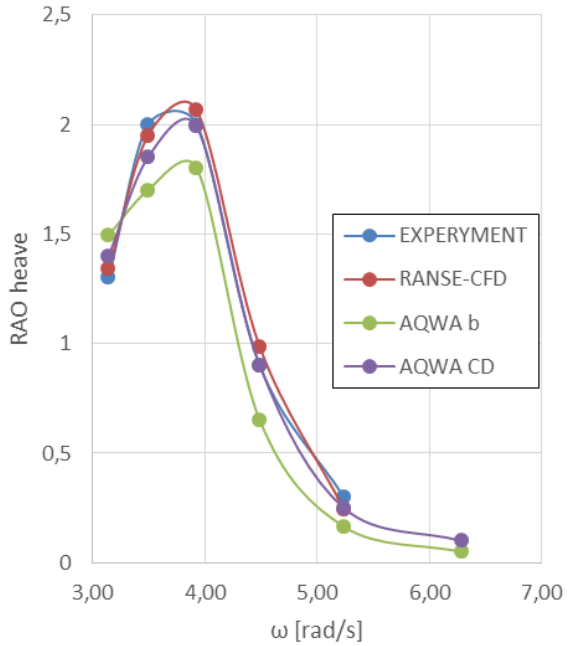

Fig. 17. Response amplitude operator for solid plates

Comparing the transfer functions obtained in the experiment for the structure with a solid plate vis-à-vis those for a plate with holes (Fig. 19), we can see that the maximum displacement for a plate with holes is smaller than that for a solid plate. Cutting holes in the plate also transfers the maximum response towards higher wave frequencies.

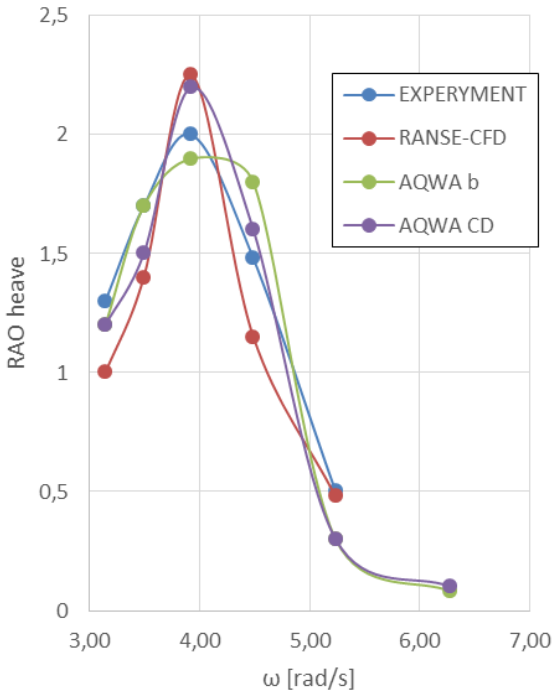

Fig. 18. Response amplitude operator for plates with holes

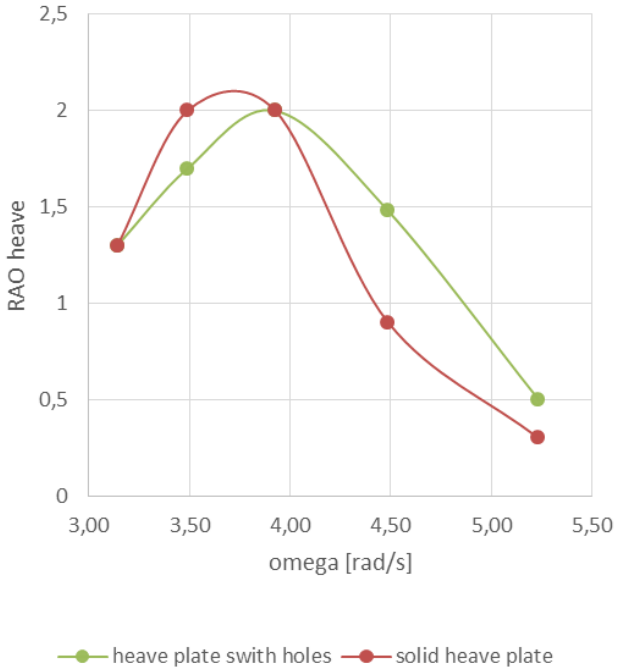

Fig. 19. Comparison of RAO for a solid and plate with holes

6. CONCLUSIONS

On the basis of the calculations carried out for the structure with a solid heave plate and a heave plate with holes, several conclusions can be drawn. The use of a heave plate results in an increase in both inertia and damping forces as compared with a

smooth cylinder. This is related to the increase in the added mass and the increase in the dissipation of energy flowing from the edge of the vortex plate. Cutting holes in the damping plate reduces the weight of the added mass in relation to the solid plate, while maintaining significant damping.

The hydrodynamic coefficients change both depending on the excitation frequency and the amplitude of the structure movement. In the case of the linear damping factor, these changes are much more pronounced than in the case of the quadratic damping factor. Therefore, when modelling the movement of the structure in a program based on the diffraction method, where the influence of viscosity is modelled with a constant linear or quadratic damping factor, a better solution is to choose a quadratic damping factor. The problem of modelling the value of the damping coefficient depending on the amplitude of the structure motion should be solved by determining its value at the expected maximum amplitude of the structure motion in operating conditions. It should be remembered that such a solution may result in underestimated displacements of the structure on waves in the remaining frequency range.

Performing a comparison between the transfer functions obtained for a structure with solid heave plates vis-à-vis those corresponding to heave plates with holes shows that cutting out the holes can reduce the maximum displacement of the structure in the wave. Cutting holes also shifts the transfer function towards higher wave frequencies. The use of a solid plate or a plate with holes for a specific structure should be decided after comparing the course of the transfer function with the expected spectrum of an irregular wave in the area of its operation.

REFERENCES

1. Dymarski P, Dymarski C, Ciba E. Stability Analysis of the Floating Offshore Wind Turbine Support Structure of Cell Spar Type During its Installation. Polish Maritime Research 2019, Vol. 26, 4(104), 109-116. DOI:10.2478/pomr-2019-0072.
2. Kraskowski M, Marcinkowski T. Numerical and experimental analysis of the wave induced forces on the tripod support structure. Laboratory study. Bulletin of Maritime Institute in Gdańsk 2017 32(1):21-29. DOI 1 0.5604/12307424.1224269.
3. Motallebi M, Ghassemi H, Shokouhian M. DeepCwind semi-submersible floating offshore wind turbine platform with a nonlinear multi-segment catenary mooring line and intermediate buoy. Scientific Journals of the Maritime University of Szczecin 2022, 69 (141). DOI: 10.17402/496.
4. Ciba E, Dymarski P, Grygorowicz M. Heave Plates with Holes for Floating Offshore Wind Turbines. Polish Maritime Research 2022 vol 29 pp.26-33. DOI: 10.2478/pomr-2022-0003.
5. Subbulakshmi A, Sundaravadivelu R. Heave damping of spar platform for offshore wind turbine with heave plate. Ocean Engineering 2016 121, 24-36.
6. Tao L, Cai S. Heave Motion Suppression of a Spar with a Heave Plate. Ocean Engineering 2004.
7. Medina-Manuel A, Botia-Vera E, Saettone S, Calderon-Sanchez J, Bulian G, Souto-Iglesias Hydrodynamic coefficients from forced and decay heave motion tests of a scaled model of a column of a floating wind turbine equipped with a heave plate. Ocean Engineering 2022,252. https://doi.org/10.1016/j.oceaneng.2022.110985.
8. Ciba E. Heave Motion of a Vertical Cylinder with Heave Plates. Polish Maritime Research 2021, Vol. 28,iss. 1(109), s.42-47 .https://doi.org/10.2478/pomr-2021-0004.
9. Tao L, Dray D. Hydrodynamic performance of solid and porous heave plates. Ocean Engineering 2008. doi:10.1016/j.oceaneng.2008.03.003.
10. An S, Faltinsen O.M. An experimental and numerical study of heave added mass and damping of horizontally submerged and perforated rectangular plates. Journal of Fluids and Structures 39 (2013) 87-101
11. Tian X. et al Hydrodynamic coefficients of oscillating flat plates at 0:15 < KC < 3:15. Journal of Mechanical Science and Technology 2016. https://doi.org/10.1016/j.apor.2019.102042.
12. Mentzoni F, Kristiansen T. Two-dimensional experimental and numerical investigations of parallel perforated plates in oscillating and orbital flows. Applied Ocean Research. 2020. 10.1016/j.apor.2019.102042.
13. Molin B, On the added mass and damping of periodic Arrays of fully or partially porous disks. Journal of Fluid and Structures 2001, 15(2), 275-290. doi:10.1006/jfls.2000.0338.
14. Mojtaba E, Tao L, Shabakhty N. Hydrodynamic damping of solid and perforated heave plates oscillating at low KC number based on experimental data: A review. Ocean Engineering 2022. DOI: 10.1016/j.oceaneng.2022.111247.
15. Rao MJ, Nallayarasu S, Bhattacharyya SK. Numerical and experimental studies of heave damping and added mass of spar with heave plates using forced oscillation. Applied Ocean Research 2021, 111. https://doi.org/10.1016/j.apor.2021.102667.
16. Maron A, Fernandez EM, Valea A, Lopez-Pavon C. Scale Effects on Heave Plates for Semi-Submersible Floating Offshore Wind Turbines. Case Study With a Solid Plain Plate. Journal of Offshore Mechanics and Arctic Engineering 2019. DOI: 10.1115/1.4045374.
17. Raed K, Murali K, Experimental and numerical analysis of a spar platform subjected to regular waves, Developments in Maritime Technology and Engineering – Guedes Soares & Santos (eds) 2021. DOI: 10.1201/9781003216599-64.

Ewelina Ciba: https://orcid.org/0000-0002-9042-5234
Paweł Dymarski: https://orcid.org/0000-0002-6033-0461